Saudi Pharmaceutical Journal 32 (2024) 101992

HOSTED BY

ELSEVIER

Contents lists available at ScienceDirect

Saudi Pharmaceutical Journal

journal homepage: www.sciencedirect.com

New flavonoids with multiple bronchodilator activity pathways from *Tephrosia purpurea* L. (Pers.) growing in Saudi Arabia

Maged S. Abdel-Kader [a,b,*], Abdulaziz S. Saeedan [c], Najeeb U. Rehman [c], Hayder M. Faqihi [d], Gamal A. Soliman [c,e]

[a] *Department of Pharmacognosy, College of Pharmacy, Prince Sattam bin Abdulaziz University, Al-Kharj 11942, Kingdom of Saudi Arabia*
[b] *Department of Pharmacognosy, College of Pharmacy, Alexandria University, Alexandria 21215, Egypt*
[c] *Department of Pharmacology and Toxicology, College of Pharmacy, Prince Sattam bin Abdulaziz University, Al-Kharj 11942, Kingdom of Saudi Arabia*
[d] *Faqihi Commercial Institution, Ahad Al Masariha Governorate, Jizan 86646-6442, Kingdom of Saudi Arabia*
[e] *Department of Pharmacology, College of Veterinary Medicine, Cairo University, Giza, Egypt*

ARTICLE INFO

Keywords:
Tephrosia purpurea
Tephropurpugazanin
Epi-Tephroapollin
Guinea pigs
Bronchodilator
Ex-vivo
In-vivo

ABSTRACT

Total extract of *Tephrosia purpurea* (*T. purpurea*) expressed potent *ex-vivo* bronchodilator effect in isolated Guinea pigs' tracheal muscles. Fractionation of *T. purpurea* total extract (**TPTE**) using liquid–liquid technique followed by *ex-vivo* bronchodilator testing indicated that the activity was trapped to the chloroform ($CHCl_3$) soluble fraction. Phytochemical study of the $CHCl_3$ fraction guided by *ex-vivo* bronchodilator activity led to the isolation of 7 active flavones of which compounds **1** (*epi*-Tephroapollin G), **3** (Acetyltephroapollin C), **4** (4''-Dehydroxytephroapollin E), and **5** (*epi*-Tephroapollin F) were new. Structures were identified using relevant spectroscopic tools including optical rotations and CD data. Compounds **1**, **3**, **4** and lanceolatin A (**6**) behaved like papaverine by inhibiting carbachol (CCh) as well as high potassium (K^+)-mediated contractions at equivalent concentrations with varied potencies whereas (-)-Tephroapollin G (**2**) selectively inhibited CCh-mediated contractions but was not found active against high K^+. *epi*-Tephroapollin F (**5**) and (-)-Pseudosemiglabrin (**7**) in contrast were significantly more potent to abolish CCh induced contraction when compared with high K^+ similar to dicyclomine. Papaverine like dual phosphodiesterase enzyme Ca^{++} ion inhibitory activities of **1, 3, 4** and **6** were confirmed indirectly by the bolster of the isoprenaline curves against CCh to the left whereas Ca^{++} inhibitory effect of **1** and **3**–**7** was confirmed by the rightward deflection of Ca^{++} concentration–response curves (CRCs) towards right with quashing of the maximum response in same fashion like verapamil. Moreover, compounds **2, 5** and **7** at lower concentrations showed selective blockade of muscarinic receptor similar to atropine. Oral administration of the **TPTE**, $CHCl_3$ and **7** to guinea pigs significantly protected against bronchospasm induced by 0.2 % histamine aerosol *in vivo*.

1. Introduction

The genus *Tephrosia* family Fabaceae includes about four hundred species broadly spread in both the eastern and western hemispheres in the tropical, subtropical and arid regions (Chen et al., 2014; Stevenson et al., 2012; Touqeer et al., 2013;Weakley, 2012). Members of the genus rang from upright herbs to soft or woody shrubs developed to 0.5–4 m height. The plants can fix nitrogen hence regenerate soil fertility (Roark, 1937; Stevenson et al., 2012). Because the dense trichomes the members of the genus gave greyish tint and were names τεφρος (tephros) in Greek meaning "ash-colored" (Umberto, 2000). This genus is represented in Saudi Arabia by about 11 species (Chaudhary, 2001; Collenette, 1999; Migahid, 1989). Tephrosia purpurea is an erect with woody cylindrical stems near the ground, frequently covered with stiff coarse reddish hairs. This annual or perennial shrub can reach a height of 40–80 cm (Heuzé V. et al., 2018).

In Unani medicine, *T. purpurea* is reported to treat kidney illnesses, cough, asthma, pain, inflammation, vomiting, boils, acne, dyspepsia, hemorrhoids, skin disorders and wounds. It has also been reported to possess laxative, diuretic insecticidal, piscicidal, and vermifuge activities (Ansari and Jahan, 2019). The plant is also used traditionally to treat jaundice, hepatomegaly, poisoning, abdominal swelling, and

* Corresponding author at: Department of Pharmacognosy, College of Pharmacy, Prince Sattam bin Abdulaziz University, Al-Kharj 11942, Saudi Arabia.
E-mail address: m.youssef@psau.edu.sa (M.S. Abdel-Kader).

https://doi.org/10.1016/j.jsps.2024.101992
Received 14 December 2023; Accepted 11 February 2024
Available online 15 February 2024

splenomegaly (Palbag et al., 2014). Pharmacological studies of *T. purpurea* indicated that the plant possesses estrogenic, antitumor, antimicrobial, antiviral, antiprotozoal, antifeedant, anti-oxidant, analgesic, anti-inflammatory, antihyperglycemic, antilipidperoxidative, antiallergic, antiulcer, anti-epileptic, hepatoprotective, nephroprotective, anxiolytic, membrane stabilizing potency, wound healing, immunomodulatory and spasmolytic activities (Chen et al., 2014; Patil et al., 2011).

The use of herbal mixture composed of *T. purpurea* and *Launaea intybacea* for the management of respiratory disorders was documented (Faqihi, 2016). The methanol extract of the whole *T. purpurea* plants expressed concentration-dependent relaxant effect on isolated rabbit jejunum preparations, isolated rabbit tracheal preparations and rabbit aorta preparations indicating the beneficial effect of the plant in treating gastrointestinal spasm, asthma and hypertension (Janbaz et al., 2013).

Phytochemical studies of the genus members revealed that flavonoids are the major secondary metabolites present in *Tephrosia*. Considerable numbers of these flavonoids belong to the rare 5-deoxy flavonoids class. Additionally, very few triterpenes and sesquiterpenes were identified from this genus (Chen et al., 2014). Analysis of the different parts of *T. purpurea* yielded of more than 44 composites belonging to different classes where more than 32 flavonoids isolated contained the rare prenylated 5-deoxyflavonoids such as lanceolatin A, semiglabrin and semiglabrinol (Rao et al., 2020).

The current phytochemical study directed by bronchodilator effect resulted in the structure identification as well as demonstrating the mechanism of action of the active components present in the plant extract of *T. purpurea* using both *ex-vivo* and *in-vivo* methods.

2. Materials and methods

2.1. General

Measurements of the melting points were done with Thermosystem FP800 Mettler FP80 instrument manufactured by Mettler-Toledo (USA) equipped with FP81 MBC cell apparatus.

Ultraviolet spectral data were obtained using Unicum Heyios a UV–Visible spectrophotometer (Thermo Fisher Scientific, USA).

By using a Bruker spectrometer (UltraShield Plus 500 MHz) and the standard manufacturer software (Switzerland) at frequency of 500 MHz for protons (^{1}H) and 125 MHz for carbon atoms (^{13}C), respectively, ^{1}H, ^{13}C NMR and 2D-NMR (COSY, HSQC, H2BC and HMBC) experiments were accomplished. Chemical shifts are given in δ parts per million (ppm) correlated with undeuterated solvents peaks, while J values (coupling constant) are reported in Hertz (Hz).

High Resolution Electrospray Ionization Mass Spectrometry (HRESIMS) were performed by UPLC RS Ultimate 3000-Q Exactive hybrid quadrupole-Orbitrap mass spectrometer manufactured by Thermo Fisher Scientific (USA), equipped with a high-resolution quadrupole precursor selection, and accurate mass (HR/AM) Orbitrap™ detection. Samples were lyophilized using Millroch laboratory freeze dryer LD85 (USA) prior to be separated medium-pressure liquid chromatography (MPLC) system equipped with pump (Buchi C-605), control unit (Buchi C-620) fraction collector (Buchi C-660), and UV photometer detector (Buchi C-640). Column 15/460–044032 was used under Sepacore software (Switzerland). Silica gel particle size 60/230–400 mesh from Merck company (USA), sephadex LH-20 from Amersham company (Sweden), RP C-18 silica gel particle size 40–63/230–400 mesh from Fluka were employed for column chromatographic separations. Thin-layer chromatography was conducted using Kiesel gel 60 F254 and RP-18 F254 plates from Merck (USA) and spot detection was achieved using CN-15-MC UV lamp operating at 254 nm (France).

2.2. Plant materials

In November 2016, *Tephrosia purpurea* L. (Pers.) were collected from Gazan, Southern part Saudi Arabia. The collected plants authentication was confirmed by Dr. Mona Alwahibi, Botany and Microbiology Department at the College of Science, KSU, Riyadh, SA. A voucher specimen (#MSA 10521) preserved at the Department of Pharmacognosy, College of Pharmacy, PSAU.

2.3. Extraction and isolation

The aerial parts were dried powdered and extracted multiple times using 95 % ethyl alcohol. The combined solvent was removed under vacuum using evaporator adjusted to 40 °C giving 53 g residue'**TPTE"**. A portion of the **TPTE** was suspended in (800 mL) ethanol containing 40 % water and partitioned with the following solvents: Petroleum ether (3 x 500 mL) to gain 13.45 g petroleum ether fraction (**Pet Ether**); **$CHCl_3$** (4 x 500 mL) to obtain 14.12 g **$CHCl_3$**; ethyl acetate (2 x 400 mL) to gain 23.30 g ethyl acetate soluble part (**EtOAc**); finally the remaining aqueous phase was freeze dried giving 0.4 gm (**Aqueous)**.

From the $CHCl_3$ part 12 g were purified on column (150 × 5 cm i.d., 300 g silica gel) using $CHCl_3$ and a gradient of $CHCl_3$/MeOH mixtures as eluent. Fractions were collected and screened by TLC. Fractions of 200 mL with similar TLC profiles were combined into fractions **A-E.**

Fraction **A** was purified over RP C-18 MPLC (45 cm X 1 cm id) using a gradient of water/MeOH mixtures (40 %- 100 %). Fractions 16–22 (49 mg) were purified further on PTLC using $CHCl_3$/MeOH (9.5:0.5) to obtain 9 mg **tephropurpugazanin** (Abdel-Kader et al., 2021) and 19 mg **compound 1** (Fig. 1-2). Similar treatment of fractions 30–45 (65 mg) led to the isolation of 11 mg of **(-)-tephropurpulin** A (Abdel-Kader et al., 2021) and 44 mg of **compound 2**. Fractions 47–48 also yielded **compound 3** after crystallization from methanol. Fractions 50–55 (35 mg) treated by PTLC with $CHCl_3$/MeOH (9.5:0.5) eluent to get 6 mg from **4''-hydroxyapollinin** (Abdel-Kader et al., 2021) and 21 mg of **compound 4**.

Fraction **B** (0.5 g) eluted with the mobile phase composed of $CHCl_3$/MeOH (9.5:0.5) was purified on column (45 cm X 1 cm id, 40 gm silica gel) with a gradient of EtOAc in petroleum ether (25 %-60). Fractions eluted with EtOAc/petroleum ether 3:7 were further fractionated on column (30 cm X 1 cm id, 15 gm RP18 silica gel) using 35 % water/MeOH mixtures, yielding 42 mg of ***epi*-Tephroapollin E** (Abdel-Kader et al., 2021) after crystallization from methanol. The supernatant liquid was purified on PTLC using mobile phase composed of $CHCl_3$/MeOH (9.5:0.5) yielding 12 mg of **compound 5**. Fractions eluted with 50 % ethyl acetate (165 mg) were crystallized from methanol, yielding 57 mg of **compound 6**. Fractions eluted with 60 % ethyl acetate (250 mg) were crystallized from methanol, yielding 185 mg of **compound 7**.

2.4. Pharmacological study

2.4.1. Animals

Guinea pigs of both sexes weighing 500–550 g were obtained from the KSU animal facility. They were accommodated at the Unit located at the College of Pharmacy, Prince Sattam bin Abdulaziz University (PSAU), in a restrained environment at 23–25 °C and had unlimited admission to standard commercial meal and running water *ad libitum*. All procedures pursued the regulations of the Institute of Laboratory Animal Resources, Commission on Life Sciences, National Research Council (NRC) (Clark et al., 1997). The study received approval number BERC-001–12-19 from the Bio-Ethical Research Committee (BERC) at PSAU.

2.4.2. Ex vivo study

2.4.2.1. Tissue preparation. Guinea pigs were euthanized by cervical dislocation, and the dissected trachea was immersed in ice-cold Krebs–Henseleit solution. The solution was bubbled with carbogen gas (95 % O_2 and 5 % CO_2 mixture) at 37 °C (Venkatasamy and Spina,

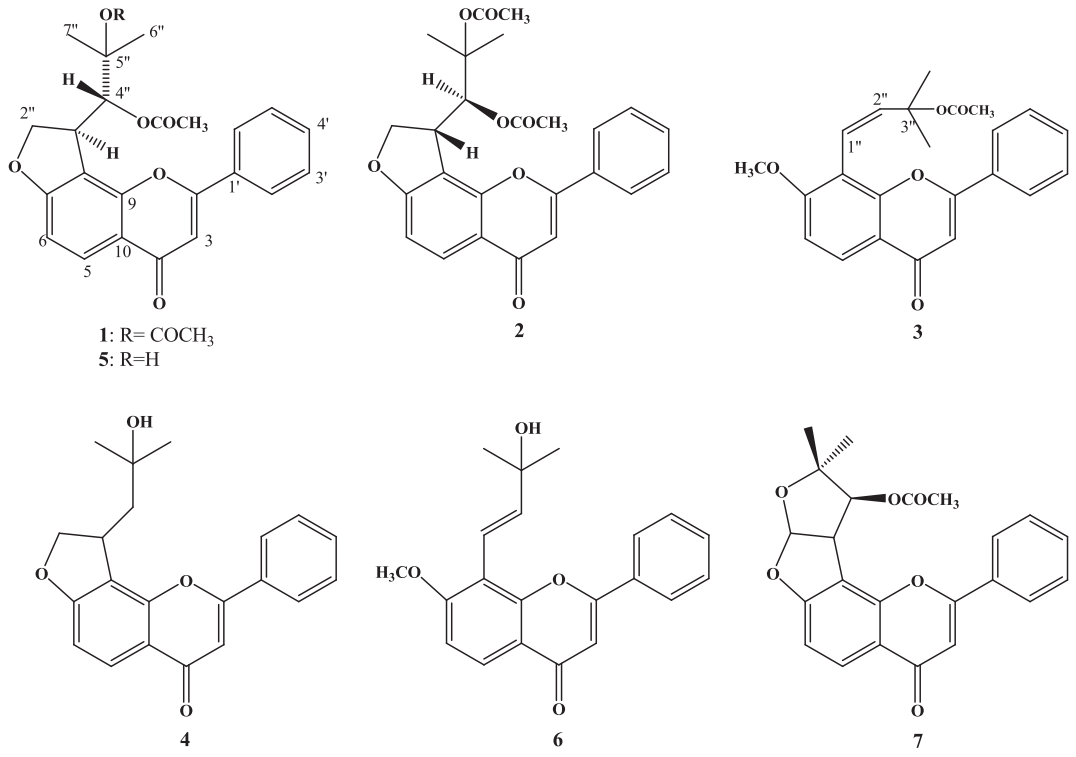

Fig. 1. Chemical compositions for flavonoids **1**–**7**.

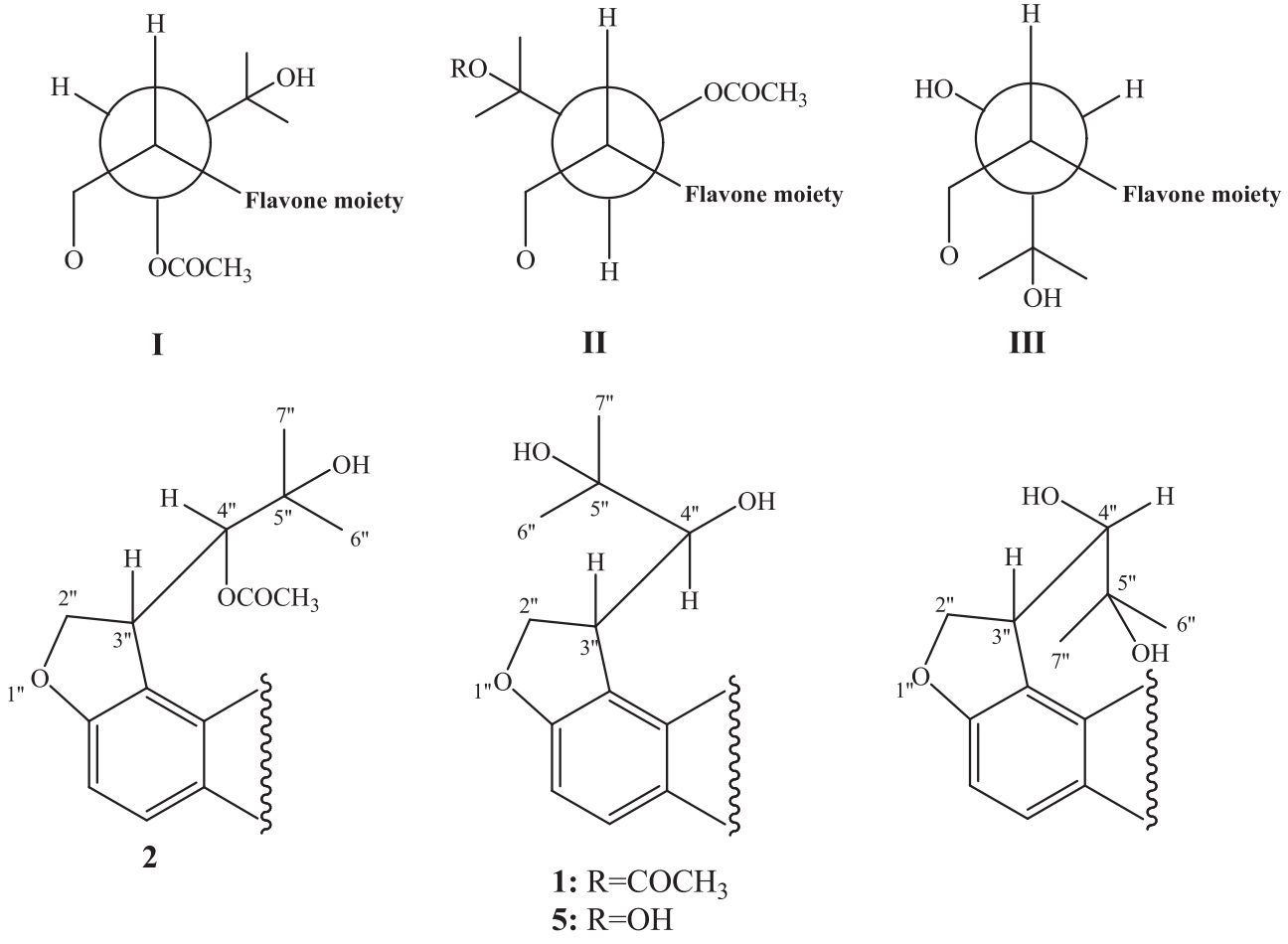

Fig. 2. Possible conformers of compounds **1**, **2** and **5**.

2016). The tracheal tissues were cleaned from adherent tissues and were cut into rings of 2 to 3-mm width. These rings were opened opposite the tracheal muscle, joined together forming a tracheal chain (Rossu, 1963), and then placed in an organ bath (20 mL volume) containing Kreb's solution. Bath temperature was set at 37 °C and carbogen gas was used for aeration. A constant tension during the whole experiment of 1 g was put in each tracheal strip.

2.4.2.2. Experimental procedure. After an equilibration period lasting a minimum of 60 min, the experimental preparations underwent testing by developing contraction using CCh (1 μM) and histamine (10 μM). These tests were conducted repeatedly employing an isometric force transducer. The system was controlled by the emkaBATH data accession software (France). When a stable tonic contraction was achieved, the plant materials were then introduced into the bath in a concentration-dependent manner using the cumulative method to evaluate their bronchodilator activity (Rossu, 1963).

2.4.2.3. Determination of the possible functional mode of action of the compounds. In order to investigate the potential involvement of multiple types of tracheal smooth muscle relaxant effect, the tracheal relaxation response curves of the test samples against contractions produced by CCh as well as high potassium (K^+) was compared with the inhibitory effects obtained with papaverine, binary inhibition of both PDE and calcium (Ca^{++}) channels (Imam et al., 2020), verapamil; blocker of Ca^{++} channles (Palande et al., 2015), dicyclomine, an antimuscarinic and Ca^{++} inhibitor (Downie et al., 1977) and atropine, an anti-muscarinic drug (Gilani et al., 1997).

Additional evidences for the involvement of the PDE-inhibitory-like action of the test sample was provided in an indirect way using isoprenaline-mediated suppression of CCh-induced spasms without (control) and with test material preincubation, as PDEIs are known to possess potentiating actions on the isoprenaline concentration response curves (CRCs) (Lis-Balchin et al., 1998; Lorenz and Wells, 1983).

Confirmation of the calcium channel blocking (CCB) action of the tested compounds was established through the following protocol. Tracheal muscles were left in Kreb's solution for stabilization before being subjected to calcium-free Kreb's solution incorporated with EDTA (0.1 mM) for 30 min to eject Ca^{++}. Subsequently, the solution was replaced by potassium-rich and calcium-free Kreb's solution composed of (in mM): KCl: 50, NaCl: 91.03, H_6NaO_6P: 0.32, $NaHCO_3$: 11.9, $MgCl_2$-$6H_2O$: 0.50, glucose: 5.05, and the calcium-chelating agent EDTA-$Na_2{\cdot}2H_2O$: 0.1 (Blattner et al., 1980).

Following a 30-minute incubation period in a bathing solution devoid of calcium ions but enriched with potassium ions, control Ca^{++} response curves were established. Once these control curves were obtained, tracheal rings were incubated with escalating doses from the test materials for 60 min, and the Ca^{++} curves were reassessed to perceive CCB-like actions.

To further authenticate whether the relaxation of the tracheal muscles of the test material was mediated by blockade of the muscarinic receptor, cumulative CRCs of CCh were obtained by applying its increasing concentrations. Once, the highest excitatory peak of CCh is achieved, the tracheal strips were washed with bathing medium and left for re-establishing the base-line tone. The CCh CRCs were re-determined using tracheal strips pre-incubated with escalating doses of the test material (Anwar-Ul et al., 1986; Boskabady and Khatami, 2003).

2.4.3. In vivo study

The potential anti-asthmatic activities of the **TPTE**, $CHCl_3$ fraction and compound **7** against bronchospasm produced by exposure to histamine were demonstrated in male guinea pigs (Ahuja et al., 2011; Ricciardolo et al., 2008). Overnight-fasted male guinea pigs were arbitrarily allotted to seven groups (n = 5). Prior to test samples treatment, pre-convulsion time (PCT) was measured for each animal as a result of exposure to 0.2 % w/v histamine dihydrochloride aerosol in a histamine chamber. Pre-convulsion time (PCT) was defined as the duration from aerosol exposure until the beginning of dyspnea resulting in convulsions on day 0 (T1). Once the PCT was determined, the animals were immediately placed in fresh air. After 48 h, the animals belonging to the first group (control) were given 2 % Tween 80 in distilled water at 1 mL/kg used as vehicle orally. Animals of the 2nd group were used as a reference group and were given chlorpheniramine maleate (2 mg/kg, i.p.). The 3rd and 4th groups animals were given single oral dose of the **TPTE** (200 & 400 mg/kg, respectively), while the 5th and 6th group of animals were given an oral dose of the **$CHCl_3$** (50 and 100 mg/kg, respectively). Animals of the 7th group received compound 7 orally at 50 mg/kg.

Two hours after treatments, all guinea pigs were subjected to histamine aerosol and pre-convulsion time was re-estimated (T2). Protective effect of each treatment was obtained applying the following formula:

$$\%protection = [1 - (T1/T2)] \times 100$$

T1 = Mean of pre-convulsion time without dosing the test compounds.
T2 = Mean of pre-convulsion time following dosing the test compounds.

2.5. Statistical analysis

Data were dispensed as the mean ± standard error (SEM). The median effective concentrations (EC_{50}) were also calculated. A one-way analysis of variance (ANOVA) accompanied by Dunnett's test was used to assess bronchodilator activities, with statistical remarkable set at $P < 0.05$. Curves correlating concentration to response were analyzed using non-linear regression with the GraphPad program (GraphPad, San Diego, CA, USA).

3. Results

3.1. Characterization of the isolated compounds

Epi-Tephroapollin G (**1**): White powder; m.p 129.8 ^{0}C; $[\alpha]_D^{25}$ + 39; CD $[\theta]_{275}$ + 2610, $[\theta]_{261}$ + 3548; UV λ_{max} MeOH: 256, 305 nm; ^{1}H and ^{13}C NMR spectral data (Tables 1 and 2, Figures S1-S13); HRESIMS $[M + 1]^+$

Table 1
^{1}H NMR chemical shifts in δ ppm with *J* in parentheses in Hz for **1, 2, 4, 5** and **7** in CD_3OD.

Pos.	1	2	4	5	7*
3	6.79 s	6.71 s	6.90 s	6.69 s	6.96 s
5	7.95 (d, 8.6)	7.93 *m*	7.83 (d, 8.5)	7.83 (d, 8.4)	7.99 (d, 8.6)
6	6.87 (d, 8.6)	6.83 (d, 8.6)	6.80 (overl.)	6.76 (d, 8.4)	7.00 (d, 8.6)
2′,6′	8.04 (d, 7.8)	7.93 *m*	8.03 (d, 7.4)	7.95 (d, 7.5)	8.01 (d, 7.9)
3′,4′,5′	7.55 *m*	7.54 *m*	7.57 *m*	7.44 *m*	7.58 *m*
2′'	4.78 (t, 9.2) 4.96 (d, 9.2)	4.84 (overl.) 5.15 (q, 5.6)	4.65 (t, 6.8) 4.87 (d, 9.5)	4.63 (t, 8.6) 4.86 (d, 9.6)	6.54 (d, 6.4)
3′'	4.25 (t, 8.2)	4.44 (q, 5.6)	4.04 (bq, 9.5)	4.08 (t, 8.0)	4.86 (t, 7.2)
4′'	5.35 (d, 8.5)	5.77 (d, 2.2)	1.74 (t, 12.5) 2.25 (d, 13.8)	4.91 (d, 9.0)	5.56 (d, 8.8)
Gem Me_2	1.54 s, 1.70 s	1.84 s, 1.57 s	1.21 s, 1.28 s	1.29 s, 1.17 s	1.05 s, 1.33 s
Acetyl	1.55 s, 1.97 s	1.70 s, 2.07 s		1.36 s	1.41 s

* Data were measured in DMSO.

Table 2
^{13}C NMR chemical shifts for **1, 2, 4, 5** and **7** in CD_3OD.

Pos.	1	2	4	5	7*
2	163.42	163.53	161.87	163.38	162.34
3	105.99	106.34	107.00	105.67	107.15
4	178.17	178.30	176.78	178.38	176.83
5	127.72	128.23	126.84	127.47	128.07
6	109.11	108.56	108.91	109.54	109.09
7	166.83	166.19	165.09	166.99	164.41
8	114.06	113.55	118.15	114.75	112.72
9	154.22	154.13	153.58	154.25	153.65
10	117.38	117.20	118.41	117.28	118.213
1′	131.07	131.40	132.08	131.04	131.30
2′,6′	126.21	126.11	126.49	126.21	126.67
3′,5′	128.97	128.91	129.45	128.92	129.52
4′	131.91	131.73	131.68	131.82	132.31
2′'	77.48	73.47	80.44	78.16	112.53
3′'	40.61	40.48	36.62	40.59	47.75
4′'	77.17	76.12	47.16	79.23	76.65
5′'	82.69	82.47	69.33	71.57	85.04
Gem	18.89	18.88	30.31	23.70	23.37
Me_2	20.60	21.57	31.68	26.4	27.43
Acetyl	169.58, 22.45	170.21, 22.56	–	169.87, 18.97	169.56, 20.43
	170.33, 21.08	170.27, 21.57			

* Data were measured in DMSO.

m/z 437.1593 (calcd for $C_{25}H_{24}O_7$ + H, 437.1600) (Figure S14).

(-)-Tephroapollin G (**2**): White powder; m.p 102.7 ^{0}C; $[\alpha]_D^{25}$ −157; CD $[\theta]_{335}$ + 1113, $[\theta]_{310}$ 0, $[\theta]_{261}$—3809, $[\theta]_{235}$ 0; UV λ_{max} MeOH: 256, 305 nm; ^1H and ^{13}C NMR spectral data (Tables 1 and 2, Figures S15-S22); HRESIMS $[M + 1]^+$ *m/z* 437.1591 (calcd for $C_{25}H_{24}O_7$ + H, 437.1600) (Figure S23).

Acetyltephroapollin C (**3**): Yellowish powder; m.p 122.4 ^{0}C; UV λ_{max} MeOH: 256, 317 nm; ^1H and ^{13}C NMR spectral data (Table 3, Figures S26-S33); HRESIMS $[M + 1]^+$ *m/z* 379.1537 (calcd for $C_{23}H_{22}O_5$ + H, 379.1537), $[M + Na]^+$ *m/z* 401.1354 (calcd for $C_{23}H_{22}O_5$ + Na, 401.1354), $[M-1]^+$ *m/z* 377.1371 (calcd for $C_{23}H_{22}O_5$-H, 377.1371) (Figures S34, S35).

4′'-Dehydroxytephroapollin E (**4**): White powder; m.p 155.3 ^{0}C; UV λ_{max} MeOH: 254, 308 nm; ^1H and ^{13}C NMR spectral data (Tables 1 and 2, Figures S36-S45); HRESIMS $[M + 1]^+$ *m/z* 337.1426 (calcd for $C_{21}H_{20}O_4$ + H, 337.1440), $[M + Na]^+$ *m/z* 359.1243 (calcd for $C_{21}H_{20}O_4$ + Na, 359.1259), $[M-1]^+$ *m/z* 335.1282 (calcd for $C_{21}H_{20}O_4$-H, 335.1283) (Figures S46, S47).

Epi-Tephroapollin F (**5**): yellowish powder; m.p 161.6 ^{0}C; $[\alpha]_D^{25}$ + 72.3; CD $[\theta]_{279}$ + 1407, $[\theta]_{255}$ + 3281; UV λ_{max} MeOH: 250, 311 nm ^1H and ^{13}C NMR spectral data (Tables 1 and 2, Figures S48-S54); HRESIMS $[M + 1]^+$ *m/z* 395.1487 (calcd for $C_{23}H_{22}O_6$ + H, 395.1495), $[M + Na]^+$ *m/z* 417.1304 (calcd for $C_{23}H_{22}O_6$ + Na, 417.1314) (Figures S55).

Lanceolatin A (**6**): Colourless crystals; m.p 191.7 ^{0}C; $[\alpha]_D^{25}$ −26; UV λ_{max} MeOH: 257, 314 nm; ^1H and ^{13}C NMR spectral data (Table 3, Figures S56-S63); HRESIMS $[M + 1]^+$ *m/z* 337.1428 (calcd for $C_{21}H_{20}O_4$ + H, 337.1400) (Figure S64).

(-)-Pseudosemiglabrin (**7**): Colourless crystals; m.p. 176.5 ^{0}C; $[\alpha]_D^{25}$ −404; CD $[\theta]_{340}$ 0, $[\theta]_{278}$—5011, $[\theta]_{256}$—8021, $[\theta]_{246}$—7618; UV λ_{max} MeOH: 258, 310 nm; ^1H and ^{13}C NMR spectral data (Tables 1 and 2, Figures S65-S83); HRESIMS $[M + 1]^+$ *m/z* 393.1331 (calcd for $C_{23}H_{20}O_6$ + H, 393.1338)(Figure S84).

Table 3
^1H-and ^{13}C NMR chemical shifts in δ ppm for **3** and **6**.

Pos.	3*		6**	
	^1H***	^{13}C	^1H	^{13}C
2	6.78, s	164.02	6.97, s	161.26
3	–	105.38	–	106.90
4	–	178.91	–	177.30
5	8.03 (d, 8.9)	125.26	7.94 (d, 8.8)	124.94
6	7.17 (d, 8.9)	109.36	7.26 (d, 8.8)	110.24
7	–	161.08	–	162.96
8	–	115.24	–	114.56
9	–	154.17	–	154.14
10	–	116.78	–	117.95
1′	–	131.19	–	131.95
2′,6′	7.99 (d, 7.2)	126.33	8.07 (d, 7.8)	126.90
3′,5′	7.52 *m*	128.78	7.56 *m*	129.54
4′		131.66		132.19
1′'	6.22 (d, 12.5)	116.20	6.90 (d, 16)	114.25
2′'	6.07 (d, 12.5)	139.28	6.78 (d, 16)	146.13
3′'	–	80.71	–	70.24
7-OCH_3	3.94 s	55.35	3.98 s	56.19
Gem Me_2	1.38 s	25.55	1.36 s	30.62
Acetyl	1.41 s	169.88, 20.15		

* Data were measured in CD_3OD.
** Data were measured in DMSO.
*** *J* in parentheses in Hz.

3.2. Effects of *TPTE* and its fractions on isolated tracheal strips

The **TPTE** and its **Pet Ether**, **$CHCl_3$**, **EtOAc** and **Aqueous** fractions were tested for their possible bronchodilatory effects expressed as the ability to vanish contractions resulted from CCh (1 μM) and histamine (10 μM) exposure using isolated tracheal preparations..

TPTE and its **Pet Ether** and **$CHCl_3$** fractions (0.01–3 mg/mL) inhibited CCh concentration dependent bronchospasms. **$CHCl_3$** was perceived to cause the most potent effect (0.01–1 mg/mL). Further, **EtOAc** and **Aqueous** fractions were found partially active. The mean EC50 induced by the **TPTE** was 1.322 mg/mL (1.063–1.644, n = 4) as shown in Fig. 3. Further, the $CHCl_3$ fraction showed 0.268 mg/mL (0.235 – 0.305, n = 4). Additionally, EC50 observed with **Pet Ether** was 1.06 mg/mL (0.85 – 1.02, n = 4) (Fig. 3).

Fig. 4 shows the relaxant effects of the column sub-fractions obtained from the **$CHCl_3$** against the CCh induced contraction, where sub fractions **A** and **B** showed complete relaxant effect with resultant EC_{50} values of 0.24 mg/mL (0.21 – 0.26, n = 3) and 0.07 mg/mL (0.05 – 0.09, n = 3), respectively. On the other hand, sub fractions **C**, **D** and **E** showed partial relaxant activity at their highest tested concentrations (1 mg/mL)

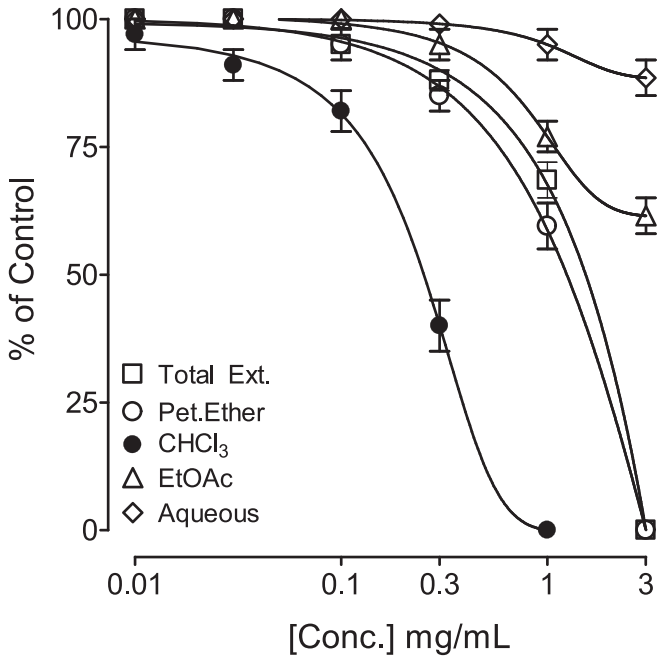

Fig. 3. Effect of **TPTE** and its **Pet. Ether**, **$CHCl_3$**, **EtOAc**, and **Aqueous** fractions on carbachol (CCh; 1 μM)-provoked guinea-pig tracheal contractions (n = 4–5).

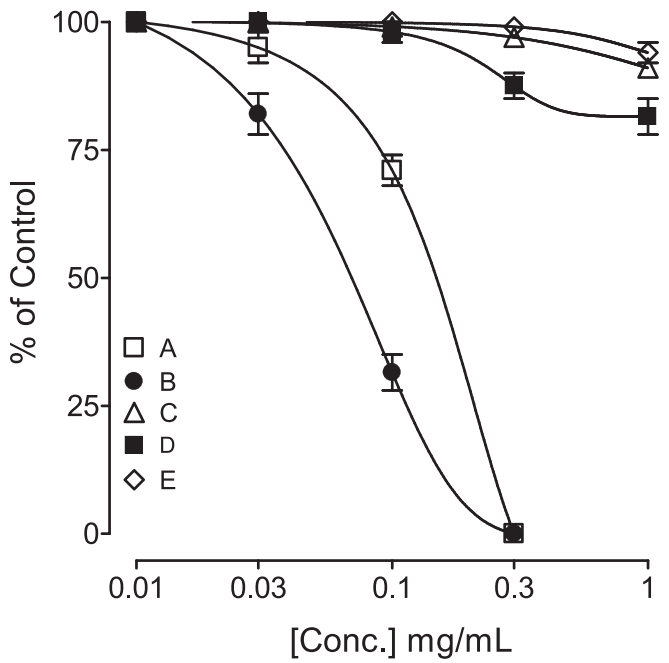

Fig. 4. Effect of column sub-fractions (**A-E**) isolated from the **$CHCl_3$** of the *T. purpurea* on carbachol (CCh; 1 μM)-provoked guinea-pig tracheal contractions (n = 4–5).

with observed maximum relaxation of 9 % **(C)**, 18.6 % **(D)**, and 6 % **(E)**, as shown in Fig. 4.

Compounds **1**–**4** have been isolated from the **$CHCl_3$** sub-fraction **A**. These compounds showed relaxant effect against CCh contraction provoked by both CCh (1 μM) as well as high K^+ (80 mM). Compound **1** showed partial but comparable inhibition against both CCh and high K^+ with resultant EC_{50} values of 0.09 mg/mL (0.07 – 1.12, n = 4) and 0.14 mg/mL (0.08 – 0.24, n = 4), respectively (Fig. 5A). Furthermore, compound **2** inhibited only CCh-mediated contractions with EC_{50} value of 0.05 mg/mL (0.04 – 0.06, n = 4) while non-significant effect ($p > 0.05$) against high K^+ (Fig. 5B). Compound **3** also expressed dual inhibition against CCh as well as high K^+ with resultant EC_{50} values of 0.008 mg/mL (0.006 – 0.009, n = 4) and 0.007 mg/mL (0.005 – 0.008, n = 4), respectively as presented in Fig. 5C. Similarly compound **4** produced dual inhibition against CCh and high K^+ with EC_{50} values of 0.07 mg/mL (0.06 – 0.08, n = 4) and 0.07 mg/mL (0.05–0.09, n = 4), respectively (Fig. 5D).

Compounds **5** and **7** obtained from sub-fraction **B** of the **$CHCl_3$** showed higher potency against CCh with EC_{50} values of 0.01 mg/mL (0.009 – 0.02, n = 4) and 0.007 mg/mL (0.005—0.009, n = 4) respectively, compared to their inhibitory effect against contractions produced by high K^+ with EC_{50} values of 0.07 mg/mL (0.05–0.09, n = 4) and 0.07 mg/mL (0.05–0. 09, n = 4) respectively (Fig. 6A, C). Compound **6** oppose CCh and high K^+ action at equivalent concentrations with respective EC_{50} values of 0.005 mg/mL (0.004–0.006, n = 4) and 0.006 mg/mL (0.005 – 0.007, n = 4) as shown in Fig. 6B.

Papaverine, inhibited bronchial contractions induced by CCh in addition to high K^+ at similar concentrations with EC_{50} values of 10.42 uM (9.58 – 11.42, n = 4) and 11.22 uM (9.68 – 12.84, n = 4) respectively (Fig. 7A). In contrast, atropine showed selective activity against CCh

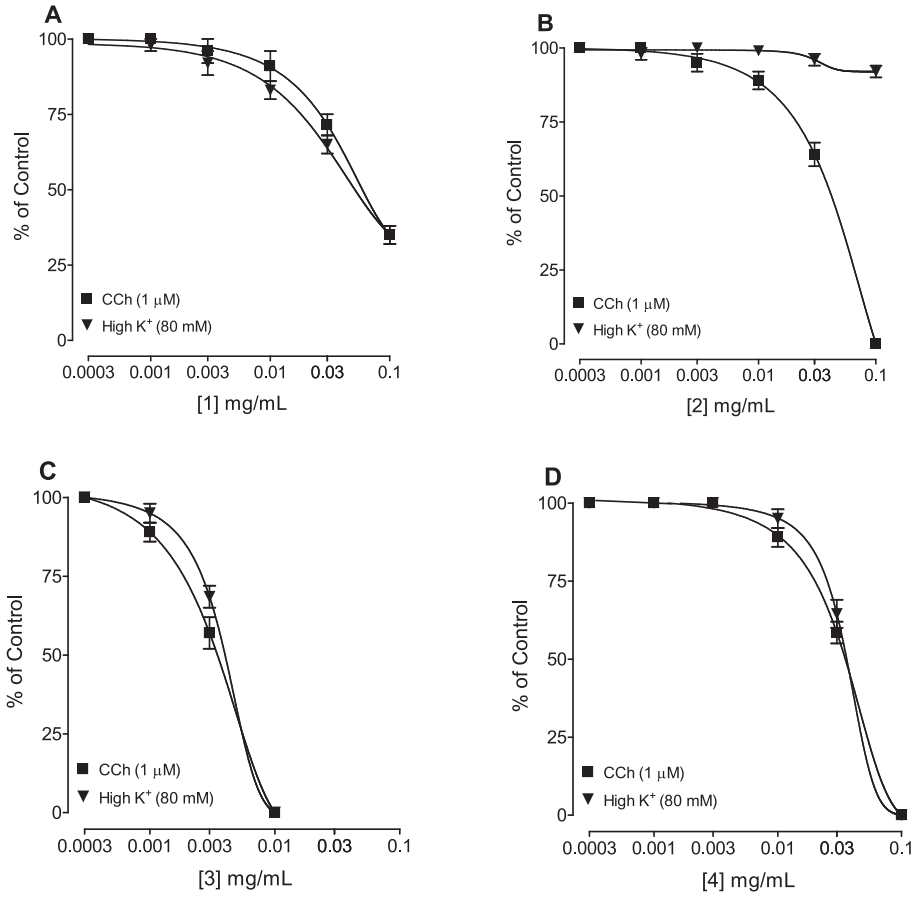

Fig. 5. Effect of compounds **1**–**4** isolated from sub-fraction **A** on carbachol (CCh; 1 μM) and high K^+ (80 mM)-induced- provoked guinea-pig tracheal contractions. Symbols represent mean ± SE; n = 4–5. **A** (compound **1**), **B** (compound **2**), **C** (compound **3**) and **D** (compound **4**).

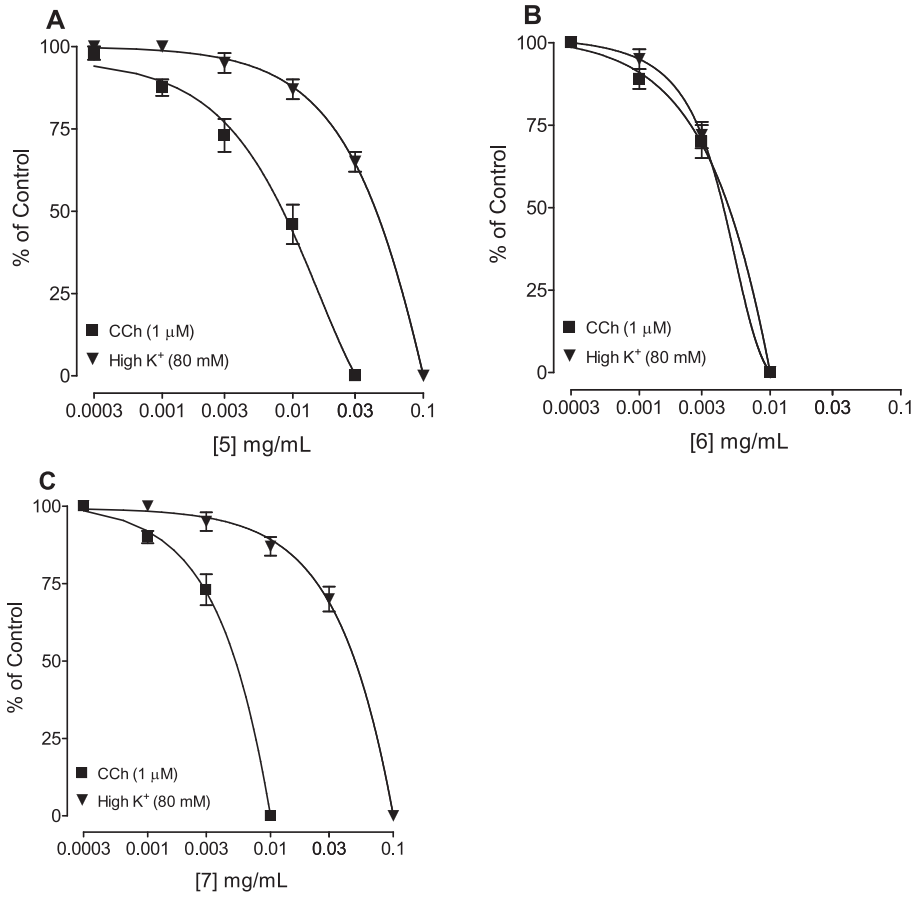

Fig. 6. Effect of compounds **5**–**7** isolated from sub-fraction **B** on carbachol (CCh; 1 μM) and high K^+ (80 mM)-provoked guinea-pig tracheal contractions. Symbols represent mean ± SE; n = 4–5. **A** (compound **5**), **B** (compound **6**) and **C** (compound **7**).

without affecting high K^+ (Fig. 7B). Dicyclomine showed stronger effect against CCh-provoked contractions in comparison to high K^+ with EC_{50} values of 1.22 uM (0.86 – 1.42, n = 4) and 10.64 uM (9.87–11.36, n = 4) respectively (Fig. 7C) while verapamil exhibited greater effect on high K^+ in comparison to CCh with observed EC_{50} values of 0.54 uM (0.46 – 0.62, n = 4) and 8.52 uM (7.92 – 10.38, n = 4) respectively (Fig. 7D). Fig. 8.

The PDE-inhibitory activity was confirmed indirectly for compounds **1**, **3**, **4 and 6** when the pre-incubation of different concentration of these compounds shifted the isoprenaline CRCs towards left and thus show potentiation similar to papaverine whereas compounds **2, 5** and **7** did not produced any significant shift (Fig. 9).

The Ca^{++} channel blocking activity was further confirmed for compounds **1**, **3**, **4**–**7** when the pre-incubation of different concentration of these compounds shifted the calcium CRCs to right side with reduction in the maximum response in the same fashion as verapamil, papaverine and dicyclomine (Fig. 9).

The antimuscarinic effect of compound **2** was further confirmed when it deflected CCh CRCs towards right in a parallel manner at both tested concentrations of 0.003 and 0.01 mg/mL (Fig. 10A) similar to atropine (Fig. 10D) whereas compounds **5**, and **7** comparable to dicyclomine at their lower concentrations expressed parallel shift in CCh CRCs while non-parallel shift in CCh CRCs was noticed at higher incubated concentrations of 0.003 mg/mL (Fig. 10B and C, respectively) similar to non-parallel shift by high doses of dicyclomine (1 uM) (Fig. 10E) whereas non-parallel shift in CCh CRCs was perceived with both lower and higher concentrations of verapamil (Fig. 10F).

3.3. *In vivo anti-asthmatic effects*

Table 4 shows the pre-convulsive time (PCT) and % protection against bronchospasm following the challenge of all animals to 0.2 % histamine aerosol.

An intraperitoneal dose of 2 mg/kg of the reference drug (Chlorpheniramine maleate) to guinea pigs significantly prolonged the PCT (7.65 ± 0.42 min) and showed 84.16 % protection against bronchospasm induced by histamine aerosol. Similarly, **TPTE** (200 & 400 mg/kg), CHCl3 (50 and 100 mg/kg) and compound 7 (50 mg/kg) significantly prolonged the PCT and increased the % protection against histamine bronchospasm when compared to the NC group.

4. Discussion

T. purpurea is used traditionally for managing airways disorders (Ansari and Jahan, 2019). The **TPTE** was evaluated for bronchodilator effect using isolated guinea-pig tracheal strips and bioassay-guided fractions was performed to isolate the active compounds. Except **EtOAc** and **Aqueous** fractions, the **TPTE**, **Pet Ether** and **$CHCl_3$** fractions concentration-dependently inhibited CCh-induced bronchospasms and the **$CHCl_3$** was identified as the most potent. Next, the **$CHCl_3$** fraction was subjected to silica gel column to get five sub-fractions (**A – E**) where **A** and **B** were found active against CCh-induced contractions. Further purification of the bioactive fractions **A** & **B** results in the purification of **1**–**4** from **A** and **5**–**7** from **B**. The structural forms of compounds **1**—**7** were established utilizing various spectroscopic techniques of structure elucidation. Following the structure determination, a detailed pharmacological study was conduct to establish the molecular interactions that underlie the bronchodilator effect of the pure isolates.

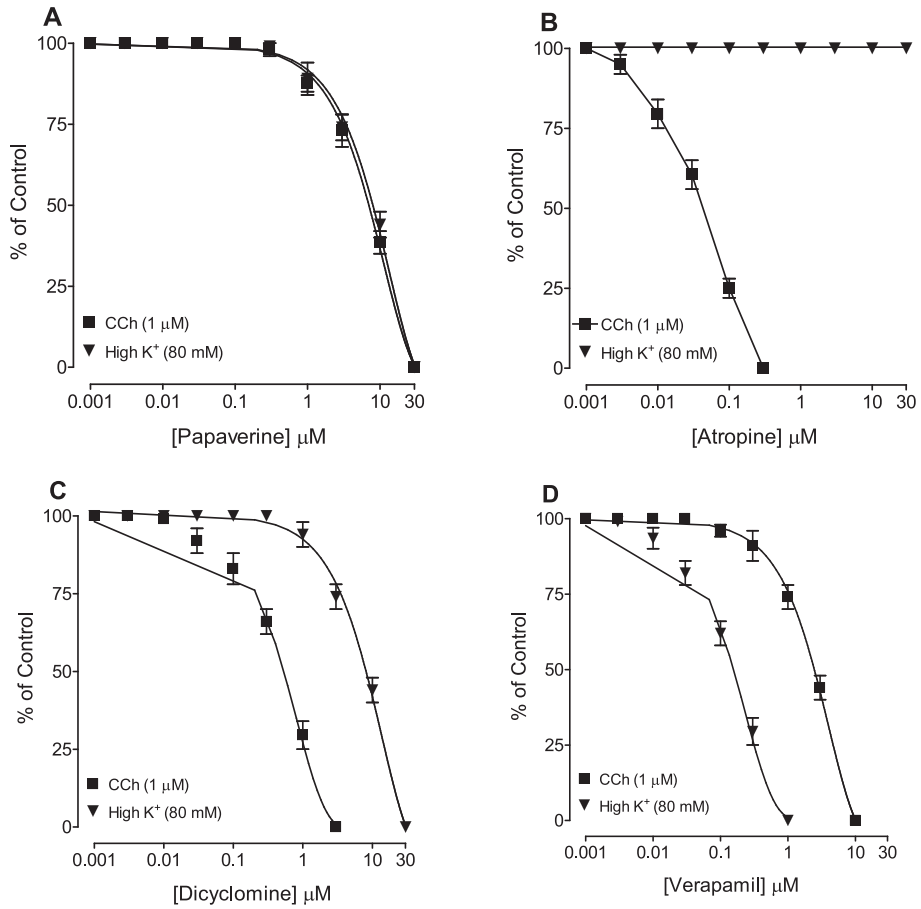

Fig. 7. Effect of papaverine **(A)**, atropine **(B),** dicyclomine **(C)** and verapamil **(D)** on carbachol (CCh; 1 μM) and high K^+ (80 mM)- provoked guinea-pig tracheal contractions (n = 4–5).

The (NMR) spectroscopy data (Tables 1-3) revealed that compounds **1**–**7** all possess a **7, 8**-disubstituted flavone skeleton Fig. 1-2). ^{1}HNMR data indicated the appearance of the 5 ring B protons in the range δ_H 7.44—8.07 ppm. The singlet at the range of δ_H 6.69—6.97 ppm were assigned for H-3 protons. Two ortho coupled doublets at the range of δ_H 7.83—8.03 and 6.76—77.76 were allocated to H-5 and H-6, respectively (Tables 1, 3). The ^{13}C NMR of the 7 compounds showed carbons signals in the range of δ_C 161.08—166.99 assigned for oxygenated C-7 (Tables 2, 3).

HRESIMS (Figures S14, S23) indicated that compounds **1** and **2** have the same molecular formula $C_{25}H_{24}O_7$. The ^{1}H NMR and ^{13}C NMR data of compounds **1** and **2** were closely similar. However, the main differences were observed in the chemical shift and *J* values of H-2″, H-3″ and H-4″ (Table 1, Figures S1-S4, Figures S15 and S16, Figure S24). The appearance of H-3″ at δ_H 4.25 (*J* = t, 8.2 Hz) and H-4″ at δ_H 5.35 (*J* = d, 8.2 Hz) indicated that compound **1** is stereoisomer of tephroapollin G **(2)** (Abd El-Razek et al., 2007). Moreover, the two compounds showed opposite sign in the optical rotation.

NMR data of compound **5** showed in addition to the flavone skeleton signals for prenyl moiety as CH_2-O, CH-O, CH, C-O and 2 X CH_3 (Tables 1, 2 and Figures S48-S54). ^{1}H NMR and ^{13}C NMR data of compound **5** pointed out to the existence of one acetyl group at δ_H 1.36 (*s*), δ_C 169.87 and 18.97 ppm. Compound **5** HRESIMS data supported the molecular formula $C_{23}H_{22}O_6$ (Figure S55) deduced from the NMR spectra. The data of compound **5** were in close agreement with those reported for tephroapollin F (Abd El-Razek et al., 2007). The main difference between tephroapollin F and compound **5** in the ^{1}H NMR was the appearance of H-3″ at δ_H 4.08 (*J* = t, 8.0 Hz) and H-4″ at δ_H 4.91 (*J* = d, 9.0 Hz) indicating that 5 has similar orientation to compound **1** rather than compound **2**. While tephroapollin F is levorotatory, compound **5** expressed dextrorotatory characters with $[\alpha]_D^{25}$ =+72.3.

Single bond usually allows free rotation unless the conformation of the compounds resulted in high energy demand to enable the free rotation. Compounds **1**, **2** and **5** exist as pure rotamer indicating that the C-3′ - C-4′ single bond has restricted rotation. Among the three possible conformer **III** is not likely to exist as the steric hindrance with the aromatic moiety will be very high. The face angle between H-3′ and H-4′ is about to 70^0 in conformer **I** reflected by the observation of H-4′ as doublet with very small *J* value of 2.2 Hz in **2** (*3″R, 4″S*). The angle between the two protons in case of conformer **II** is around 168^0 and reflected by the splitting of H-4′ to a doublet (*J* = 8.5—9.0 Hz) in **1** and **5** (*3″R, 4″R*). 3D model of the conformer **I** clarified that H-4′ is closer in space with the two equivalents H2′and H-6′ aromatic protons.

Compound **1** expressed optical rotation with positive sign (+39) in addition to signal of H-4′ at δ_H 5.35 as doublet with *J* = 8.2 Hz proving that protons H-3′ and H-4′ have "anti-conformation" as in conformer II (Abdel-Kader et al., 2021; Vleggaar & Van Aswegen, 1978). In contrast, the known compound **2** (tephroapollin G) expressed negative sign in optical rotation (−157) and H-4′′ signal as narrow doublet (*J* = 2.2 Hz) indicating the "syn orientation" of H-3′′ and H-4′′ as in conformer I (Abd El-Razek et al., 2007). The CD data of compounds **1** and **2** showed opposite sign at 261 nm. The provided data enable to confirm the identity of compound **1** as the new stereoisomer of compound **2** and was given the name *epi*-tephroapollin G. The relative configuration of compound **5** is similar to that of *epi*-tephroapollin E as they are identical in their positive optical rotation and existence of H-4′′ as doublet with *J* = 9.0 Hz (Abdel-Kader et al., 2021). Similar to **1** Compound **5** expressed negative sign in the CD spectrum at 255 nm. Consequently, compound **5**

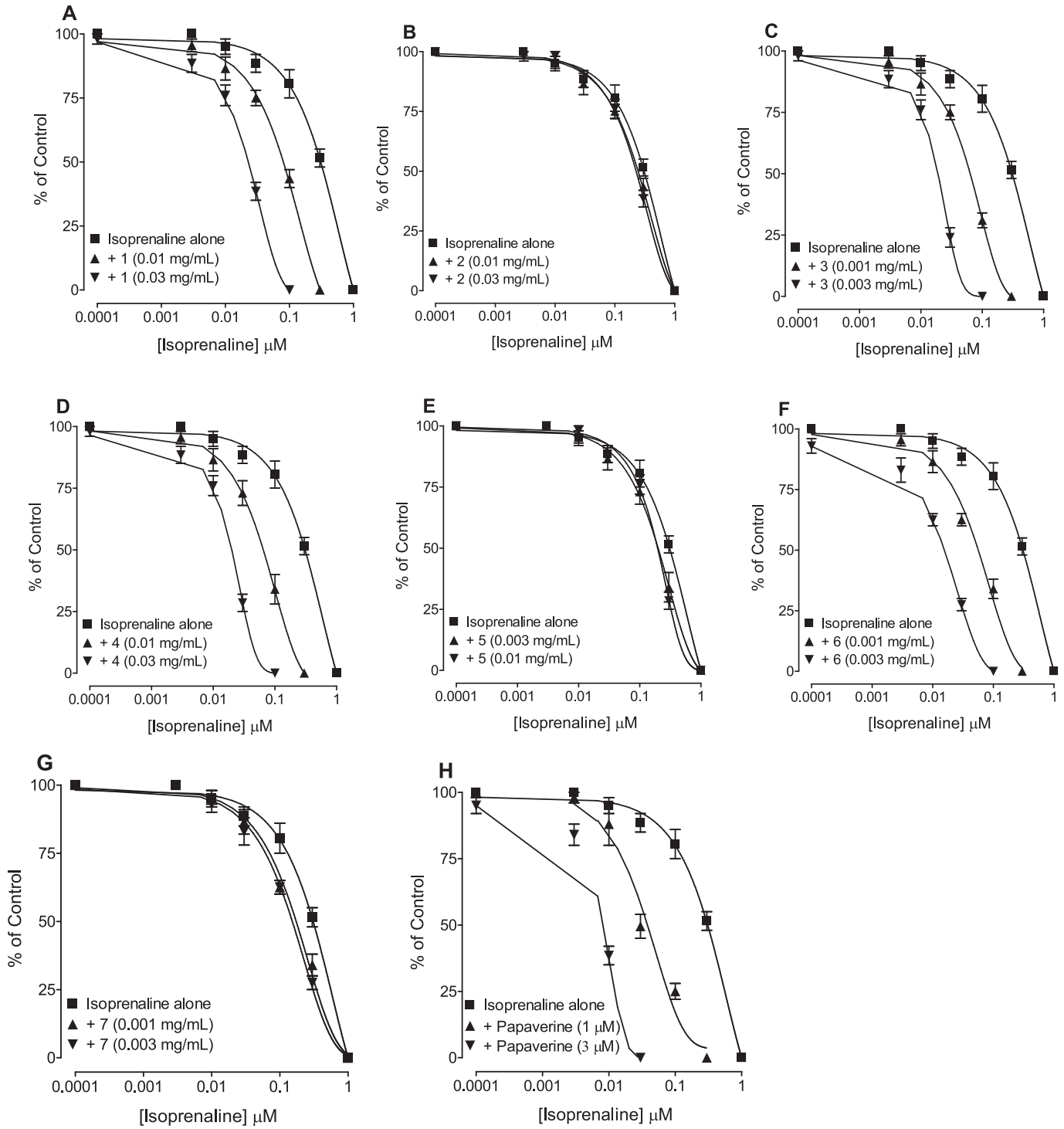

Fig. 8. The concentration–response relationships of isoprenaline against carbachol (CCh; 1 μM)- provoked guinea-pig tracheal contractions in absence and presence the increasing concentrations of **A** (compound **1**), **B** (compound **2**), **C** (compound **3**), **D** (compound **4**), **E** (compound **5**), **F** (compound **6**), **G** (compound **7**), and **H** (papaverine) (n = 4–5).

was identified as the new natural isomer *epi*-tephroapollin F.

The NMR data of compound **3** (Table 3, Figures S26- S34) showed the existence of one methoxyl group at δ_H 3.94 (s) and δ_C 55.35 ppm allocated for C-7. Five carbon signals along with their corresponding protons were assigned for prenyl moiety at C-8. The prenyl moiety signals were typical for 2-methyl but-3-en-2-ol. The *J* value 12.5 between H-1′′ and H-2′′ was diagnostic for the *cis* orientation of the double bond. The NMR data showed also signals for an acetyl moiety at δ_H 1.41(s), δ_C 169.88, 20.15 ppm. The data of compound **3** was closely related to those reported for tephroappolin C (Abd El-Razek et al., 2007). however, the latter lacks the acetyl group. The HRESIMS data of compound **3** (Figures S34 and S35) showed an $[M+1]^+$ quashi molecular ion at *m/z* 379.1537, $[M+Na]^+$ at *m/z* 401.1354 and $[M-1]^+$ ion at *m/z* 377.1371 for the formula $C_{23}H_{22}O_5$ all supporting the existence of acetyl group at C-3″ the only hydroxyl group in the compound. Compound **3** is new natural molecule and was named acetyltephroapollin C.

The HRESIMS data of compound **4** (Figures S46 and S47) showed an $[M+1]^+$ ion at *m/z* 337.1426, $[M+Na]^+$ at *m/z* 359.1243 and $[M-1]^+$

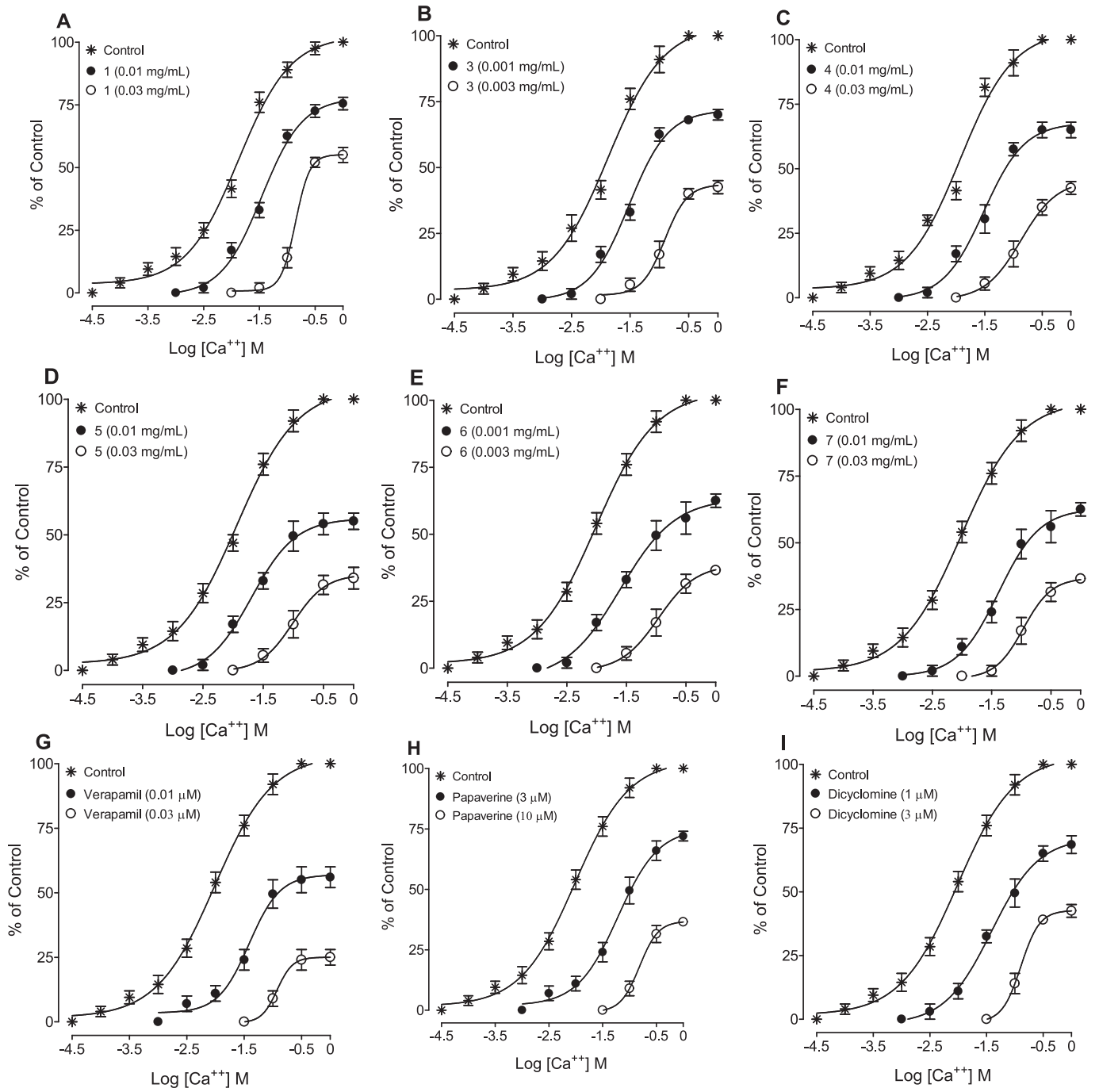

Fig. 9. The concentration–response relationships of Ca^{++} in the absence and presence of the increasing concentrations of **A** (compound **1**), **B** (compound **3**), **C** (compound **4**), **D** (compound **5**), **E** (compound **6**), **F** (compound **7**) and positive control drugs; **G** (verapamil), **H** (papaverine) and **I** (dicyclomine) in isolated guinea-pig tracheal preparations (n = 4–5).

ion at *m/z* 335.1282 representing the formula $C_{21}H_{20}O_4$. The prenyl moiety of compound **4** presented in both ^1H and ^{13}C NMR (Figures S36 and S45) by CH_2-O at δ_H 4.65 (t, 6.8 Hz), 4.87 (d, 9.5 Hz), δ_C 80.44, CH at δ_H 4.04 (bq, 9.5 Hz), δ_C 36.62, CH_2 at δ_H 1.74 (t, 12.5 Hz), 2.25 (d, 13.8 Hz), δ_C 47.16, oxygenated quaternary carbon at δ_C 69.33 and germinal dimethyl at δ_H 1.21 (s), 1.28 (s), δ_C 30.31 and 31.68 ppm. Compared with tephroapollin E compound **4** is lacking the C-4′′ hydroxyl group, a fact completely supported by the MS data. In light of the above evidences compound **4** was identified as the new natural compound 4′′-dehydroxytephroapollin E.

HRESIMS in addition to comparison with the published data enable the identification of compound **6** as Lanceolatin A and compound **7** as (-)-Pseudosemiglabrin (Waterman and Khalid, 1980).

The 7 isolates were tested in detailed for exploring the bronchodilator effect mechanisms. The 7 compounds were tested against CCh and high K^+ using the guinea-pig tracheal strips. Out of four isolated compounds from **A**, Compounds **1, 3** and **4** showed inhibition of both CCh and high K^+-mediated tracheal contractions at proportional concentrations similar to papaverine, a binary inhibitor of PDE and Ca^{++} channels (Rehman et al., 2022a). Compound **2** selectively inhibited CCh-mediated contractions but was not found active against high K^+-induced contractions similar to the effect of anticholinergic drug atropine (Rehman et al., 2022b). On the other hand, compounds **5** and **7** isolated from **B** showed inhibition against both CCh and high K^+ in a

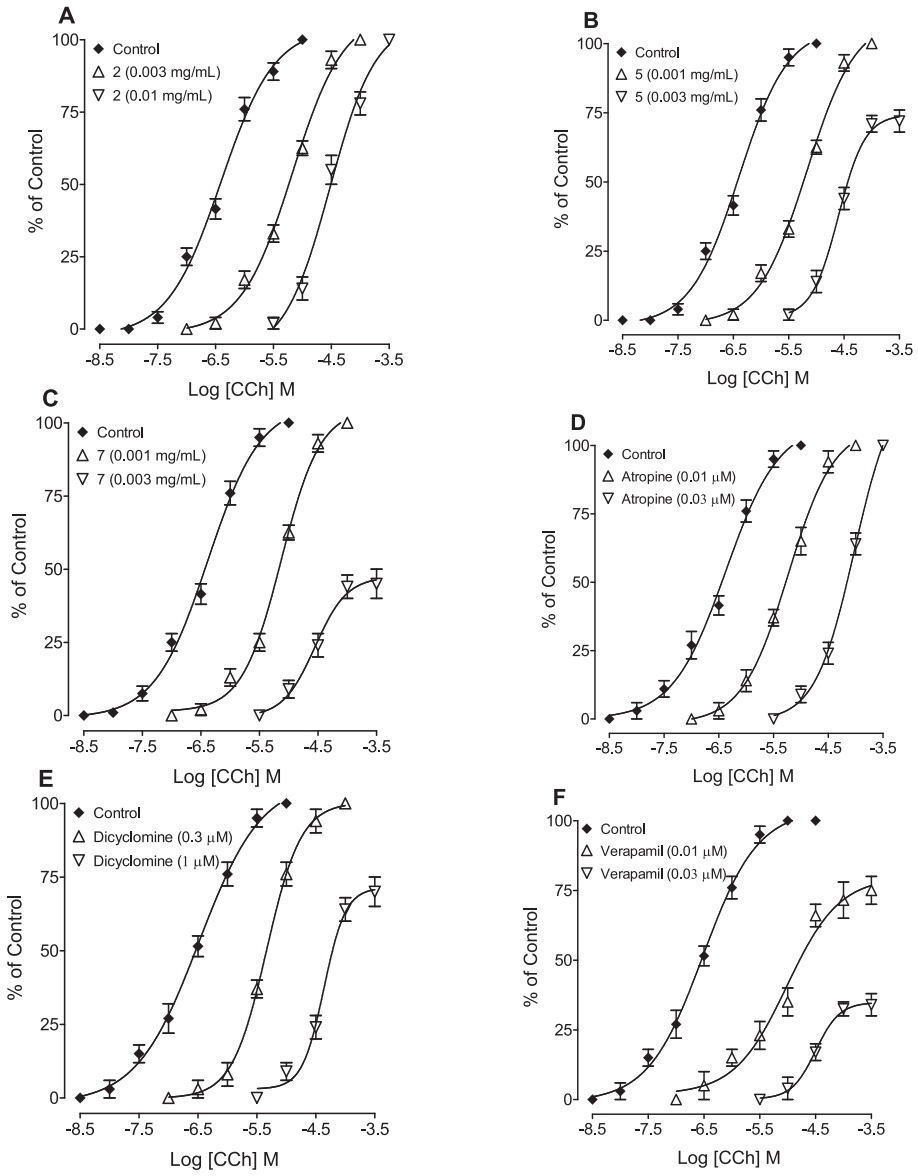

Fig. 10. The concentration–response curves of carbachol (CCh) in the absence and presence of the increasing concentrations of **A** (compound **2**), **B** (compound **5**), **C** (compound **7**) and positive control drugs; **D** (atropine), **E** (dicyclomine) and **F** (verapamil) in isolated guinea-pig tracheal preparations (n = 4–5).

fashion that were found markedly more effective against CCh compared to high K^+ thus showing predominant antimuscarinic followed by Ca^{++} inhibitory like effects similar to dicyclomine, a standard antimuscarinic and Ca^{++} channel blocker (Abdel-Kader et al., 2022). Compound **6**, being observed with equal potencies to inhibit CCh and high K^+ also behaved similar to papaverine. The papverine like dual phosphodiesterase enzyme Ca^{++} ion inhibitory-like activities of the compounds **1, 3, 4** and **6** were confirmed indirectly by the potentiation of the isoprenaline curves constructed against CCh towards left (Imam et al., 2020) whereas Ca^{++} inhibitory effect of compounds **1** and **3–7** was confirmed by the rightward deflection of calcium CRCs towards right with reduction of the ultimate response almost identical with the standard Ca^{++} channel blocker verapamil (Palla et al., 2021). Moreover, compounds **2, 5** and **7** at lower concentrations showed parallel shift in CCh CRCs towards right, a feature of a competitive antagonist, like atropine (Palla et al., 2020). Similar rightward parallel shift in CCh CRCs towards right was obtained with atropine, an anticholinergic agent (Gilani et al., 1997). Whereas, the pre-incubated tissues with higher concentrations of compounds **2, 5** and **7** showed non parallel shift in CCh CRCs towards right with inhibition of the ultimate response, thus showing non-competitive antagonist-like actions indicating the existence of non-specific suppression, as known with CCBs (Irie et al., 2000; Mitchelson and Ziegler, 1984). Dicyclomine in addition, displaced the CCh-curves toward the right side in similar fashion to these compounds, while verapamil induced rightward but non-parallel displacement with reduction of the highest contractions at both concentrations used, a typical characteristic of Ca^{++} antagonists (Irie et al., 2000; Mitchelson and Ziegler, 1984).

The cholinergic antagonists and PDE-inhibitors are known therapeutic options in the treatment of asthma (Imam et al., 2020), however, the cardiac stimulation is associated as one of their major side-effects particularly if applied orally (Nawrath, 1981). Curiously Ca^{++} antagonists are also beneficial for managing bronchoconstriction (Ahmed, 1992; Ann Twiss et al., 2002; Mathewson, 1985) but having heart depressing action (Billman, 1992). The existence of CCB-like constituent (s) alongside with anticholinergic and PDE inhibitory action in *T. purpurea* might be meant by nature to compensate tachycardia, commonly linked with PDE-inhibitors or anticholinergics if applied alone. A circumstance aligns with the idea that natural remedies possess the capacity to enhance effects or neutralize side effects, as proposed by

Table 4
In Vivo evaluation of the potential anti-asthmatic activity of **TPTE**, $CHCl_3$ fraction and compound **7** in guinea pigs exposed to histamine (n = 5).

Groups	Dose (mg/kg)	Preconvulsive time (min)		Mean exposition time (min)	% Protection
		0-time	48 h		
NC	00	1.58 ± 0.13	1.64 ± 0.11	0.06 ± 0.06	3.66
REF	2	1.44 ± 0.09	9.09 ± 0.42●	7.65 ± 0.42●	84.16
Total Ext	200	1.65 ± 0.08	6.19 ± 0.35●#	4.54 ± 0.30●#	73.34
	400	1.24 ± 0.07	16.51 ± 0.57●#	15.26 ± 0.54●#	92.43
$CHCl_3$	50	1.58 ± 0.08	6.12 ± 0.33●#	4.54 ± 0.40●#	74.18
	100	1.76 ± 0.10	7.18 ± 0.43●#	5.42 ± 0.45●#	75.49
Compound 7	50	1.34 ± 0.09	7.11 ± 0.46●#	5.77 ± 0.52●#	81.15

Values are expressed as mean ± SEM.
NC = Normal Control.
REF = Chlorpheniramine maleate.
● Significant alteration at $P \leq 0.05$ with respect to NC guinea pigs.
Significant alteration at $P \leq 0.05$ with respect to REF guinea pigs.

(Gilani, 2005). Furthermore, it underscores their cost-effectiveness and their value in evidence-based research, as noted by (Ernst, 2005).

Acute bronchospasm due to exposure to histamine aerosol in guinea pigs is highly recognized as *in vivo* model for the screening of potential anti-asthmatic efficacy of extracts or pure compounds. The used parameter is the measurement of the time taken for the development of convulsion (PCT) (Bhong Prabha et al., 2021; Shah and Parmar, 2003).

Results from *in vivo* evaluation of the anti-asthmatic efficacy of **TPTE**, $CHCl_3$ fraction and compound **7** on the bronchoconstriction resulted from exposure to histamine aerosol using guinea pigs, strongly supported the *in vitro* bronchodilatory effects. **TPTE** (200 & 400 mg/kg), $CHCl_3$ (50 and 100 mg/kg) and compound **7** (50 mg/kg) had good anti-asthmatic effects in g pigs. They significantly prolonged the PCT when compared to the NC group. **TPTE** has shown anti-asthmatic effect by attenuating responses to histamine. These effects seem regarded as its capability to inhibit PDE, block the entrance of Ca^{++} into bronchial muscles or block the muscarinic receptors at least. Increased PCT by **TPTE** expressed an inhibitory action against bronchospasm persuaded by histamine (Sing and Chakaraborthy., 2020;Krishnaraj et al., 2019).

Interestingly, the anti-asthmatic effect of **TPTE** at 400 mg/kg in guinea pigs exposed to histamine aerosols was more effective than that of the reference drug as it offers 92.43 % protection, while the reference drug produced a lower percentage of protection (84.16 %).

5. Conclusion

Phytochemical study of **TPTE** directed by bronchodilator activity resulted in the isolation and structure elucidation of 7 active flavone derivatives including 4 new compunds. The **TPTE** and the pure isolates possesses promising bronchodilator and anti-asthmatic effects mediated possibly by combination of PDE-inhibition, Ca^{++} channel blockade and muscarinic receptor antagonism while additional unexplored mechanism(s) cannot be excluded. The results provide a scientific argument to explain the usage of *T. purpurea* in traditional medicine as a remedy for bronchial disorders with the strong potential to be further developed as treatment of bronchial asthma.

CRediT authorship contribution statement

Maged S. Abdel-Kader: Conceptualization, Methodology, Investigation, Resources, Data curation, Writing – review & editing. **Abdulaziz S. Saeedan:** Conceptualization, Resources, Data curation, Writing – review & editing. **Najeeb U. Rehman:** Conceptualization, Methodology, Investigation, Data curation, Writing – original draft. **Hayder M. Faqihi:** Conceptualization, Resources. **Gamal A. Soliman:** Conceptualization, Methodology, Investigation, Writing – review & editing.

Declaration of competing interest

The authors declare that they have no known competing financial interests or personal relationships that could have appeared to influence the work reported in this paper.

Appendix A. Supplementary data

Supplementary data to this article can be found online at https://doi.org/10.1016/j.jsps.2024.101992.

References

Abd El-Razek, M.H., Mohamed, A.-E.-H.-H., Ahmed, A.A., 2007. Prenylated flavonoids from *Tephrosia apollinea*. Heterocycles: an International Journal for Reviews and Communications in Heterocyclic Chemistry 71, 2477–2490.

Abdel-Kader, M.S., Alqarni, M.H., Foudah, A.I., 2021. New Flavonoids from Saudi collection of *Tephrosia purpurea* L (Pers.). Rec. Nat. Prod. 15, 293–300.

Abdel-Kader, M.S., Rehman, N.U., Alghafis, M.A., Al-Matri, M.A., 2022. Brochodilator phenylpropanoid glycosides from the seeds of *Prunus mahaleb* L. Rec. Nat. Prod. 5, 443–453.

Ahmed, T., 1992. Calcium antagonists: Potential for asthma therapy. Choices Respir Manage 22, 41–43.

Ahuja, D., Bijjem, K.R.V., Kalia, A.N., 2011. Bronchospasm potentiating effect of methanolic extract of *Ficus religiosa* fruits in guinea pigs. J Ethnopharmacol 133 (2), 324–328.

Ann Twiss, M., Harman, E., Chesrown, S., Hendeles, L., 2002. Efficacy of calcium channel blockers as maintenance therapy for asthma. Br J Clin Pharmacol 53 (3), 243–249.

Ansari, M., Jahan, N., 2019. *Tephrosia purpurea* (L.) Pers. (Sarphuka, Wild Indigo): An important drug of Unani system of medicine. Discovery Phytomedicine-Journal of Natural Products Research and Ethnopharmacology 6.

Anwar-ul, S., Gilani, H., Cobbin, L.B., 1986. The cardio-selectivity of himbacine: a muscarine receptor antagonist. Naunyn Schmiedebergs Arch Pharmacol 332 (1), 16–20.

Bhong, P.N., Naikawade Nilofar, S., Mali Pratibha, R., Bindu Madhavi, S., 2021. In-vitro and in-vivo evaluation of anti-asthmatic activity of *Eugenia jambolana* bark. Research Journal of Pharmacy and Technology. 14 (6), 3337–13332.

Billman, G.E., 1992. The antiarrythmic effects of the calcium antagonists. Calcium Antagonists in Clinical Medicine 183–212.

Blattner, R., Classen, H.G., Dehnert, H., 1980. Experiments on isolated smooth muscle preparations. Hugo Sachs Elektronik.

Boskabady, M.H., Khatami, A., 2003. Relaxant effect of *Foeniculum vulgare* on isolated guinea pig tracheal chains. Pharm Biol 41 (3), 211–215.

Chaudhary, S.A., 2001. Flora of the Kingdom of Saudi Arabia (vascular plants). National Agriculture and Water Research Center, National Herbarium, Ministry of Agriculture and Water, Riyadh.

Chen, Y., Yan, T., Gao, C., Cao, W., Huang, R., 2014. Natural products from the genus *Tephrosia*. Molecules 19, 1432–1458.

Clark, J.D., Gebhart, G.F., Gonder, J.C., Keeling, M.E., Kohn, D.F., 1997. The 1996 guide for the care and use of laboratory animals. ILAR J 38, 41–48. https://doi.org/10.1093/ilar.38.1.41.

Weakley, A.S., 2012. Flora of the southern and mid-Atlantic states. UNC Herbarium, North Carolina Botanical Garden.

Collenette, S., 1999. Wild Flowers of Saudi Arabia, National Commission for Wildlife Conservation and Development (NCWCD). Riyadh, Saudi Arabia.

Downie, J.W., Twiddy, D.A., Awad, S.A., 1977. Antimuscarinic and noncompetitive antagonist properties of dicyclomine hydrochloride in isolated human and rabbit bladder muscle. J. Pharmacol. Exp. Ther. 201, 662–668.

Ernst, E., 2005. The efficacy of herbal medicine–an overview. Fundam Clin Pharmacol 19 (4), 405–409.

Faqihi, H.M.M., 2016. Herbal composition for treatment respiratory diseases. Saudi Patent Office, King Abdulaziz City of Science and Technology, p. 4999.

Gilani, A.H., Shaheen, F., Christopoulos, A., Mitchelson, F., 1997. Interaction of ebeinone, an alkaloid from *Fritillaria imperialis*, at two muscarinic acetylcholine receptor subtypes. Life Sci 60 (8), 535–544.

Gilani, A.H., Atta-ur-Rahman, 2005. Trends in ethnopharmacology. J Ethnopharmacol 100 (1-2), 43–49.

Heuzé V., Thiollet H., Tran G., Hassoun P., Lebas F, 2018. Ahuhu (*Tephrosia purpurea*). Feedipedia, a programme by INRAE, CIRAD, AFZ and FAO. 14–36.

Imam, F., Rehman, N.U., Ansari, M.N., Qamar, W., Afzal, M., Alharbi, K.S., 2020. Effect of Roflumilast in airways disorders via dual inhibition of phosphodiesterase and Ca2+-channel. Saudi Pharmaceutical Journal 28 (6), 698–702.

Irie, K., Yoshioka, T., Nakai, A.i., Ochiai, K., Nishikori, T., Wu, G.-R., Shibuya, H., Muraki, T., 2000. A Ca2+ channel blocker-like effect of dehydrocurdione on rodent intestinal and vascular smooth muscle. Eur J Pharmacol 403 (3), 235–242.

Janbaz, K.H., Jan, A., Qadir, M.I., Gilani, A.H., 2013. Spasmolytic, bronchodilator and vasorelaxant activity of methanolic extract of *Tephrosia purpurea*. Acta Pol Pharm 70 (2), 261–269.

Krishnaraj, S., Aathirai, K., Saravana Balaji, M.D., Premlal, K.R., 2019. *In-vitro* and *In-vivo* anti-asthmatic activity of ethanolic leaf extract of *Caesalpinia pulcherrima*. International Journal of Phytopharmacology. 10 (1), 1–5.

Lis-Balchin, M., Patel, J., Hart, S., 1998. Studies on the mode of action of essential oils of scented-leaf Pelargonium (Geraniaceae). Phytotherapy Research: an International Journal Devoted to Pharmacological and Toxicological Evaluation of Natural Product Derivatives 12, 215–217.

Lorenz, K.L., Wells, J.N., 1983. Potentiation of the effects of sodium nitroprusside and of isoproterenol by selective phosphodiesterase inhibitors. Mol Pharmacol 23, 424–430.

Mathewson, H.S., 1985. Anti-asthmatic properties of calcium antagonists. Respir Care 30, 81.

Migahid, A.M., 1989. Flora of saudi arabia: Monocotyledons. University Libraries, King Saud University, Hydrocharitaceae to Orchidaceae.

Mitchelson, F., Ziegler, A., 1984. The effect of gallamine, gallopamil and nifedipine on responses to acetylcholine and carbachol in the taenia of the guinea-pig caecum. Br J Pharmacol 83 (1), 145–155.

Nawrath, H., 1981. Action potential, membrane currents and force of contraction in mammalian heart muscle fibers treated with quinidine. J Pharmacol Exp Ther 216, 176–182.

Palande, N.V., Bhoyar, R.C., Biswas, S.P., Jadhao, A.G., 2015. Short-term exposure to L-type calcium channel blocker, verapamil, alters the expression pattern of calcium-binding proteins in the brain of goldfish. Carassius Auratus. Comparative Biochemistry and Physiology Part c: Toxicology & Pharmacology 176, 31–43.

Palbag, S., Dey, B.K., Singh, N.K., 2014. Ethnopharmacology, phytochemistry and pharmacology of *Tephrosia purpurea*. Chin J Nat Med 12 (1), 1–7.

Palla, A.H., Gilani, A.-u.-H., Bashir, S., Ur Rehman, N., 2020. Multiple mechanisms of flaxseed: Effectiveness in inflammatory bowel disease. Evid. Based Complement. Alternat. Med. 2020, 1–16.

Palla, A.H., Rehman, N.U., Siddiqi, S.H., Gilani, A.H., Siddiqui, B.S., Ilyas, M., Perwaiz, S., 2021. Cardiac depressant and vasodialatory effect of Flaxseed - basis for the medicinal use in hypertension. Sains Malaysiana 50 (9), 2687–2700.

Patil, P.V., Huger, S., Nanjappaiah, H.M., Kalyane, N., Chowdhry, M., 2011. Phytopharmacology of *Tephrosia purpurea* Linn: An Overview. Pharmacologyonline 3, 1111–1140.

Rao, A.S., Yadav, S.S., Singh, P., Nandal, A., Singh, N., Ganaie, S.A., Yadav, N., Kumar, R., Bhandoria, M.S., Bansal, P., 2020. A comprehensive review on ethnomedicine, phytochemistry, pharmacology, and toxicity of *Tephrosia purpurea* (L.) Pers. Phytother. Res. 34, 1902–1925.

Rehman, N.U., Ansari, M.N., Ahmad, W., Amir, M., 2022a. The detailed pharmacodynamics of the gut relaxant effect and GC-MS analysis of the *Grewia tenax* fruit extract: In vivo and ex vivo approach. Molecules 27 (24), 8880.

Rehman, N.U., Salkini, M.A., Alanizi, H., Alharbi, A., Alqarni, M., Abdel-Kader, M.S., 2022b. *Achillea fragrantissima* Essential Oil: Composition and detailed pharmacodynamics study of the bronchodilator activity. Separations 9 (11), 334.

Ricciardolo, F.L.M., Nijkamp, F., Rose, V.D., Folkerts, G., 2008. The guinea pig as an animal model for asthma. Curr Drug Targets 9, 452–465.

Roark, R.C., 1937. *Tephrosia* as an insecticide-a review of the literature. US Dept. of Agr. Bur. Ent. Plant Quarant., Div. Insecticide Invest. E-402.

Rossu M, V.A.N., 1963. Cumulative dose-response curve II. Techniques for the making of dose response curve in isolated organs and evaluation of drug parameters. Arch. Int. Pharmacodyn. Ther. 143, 299.

Shah, G.B., Parmar, N.S., 2003. Antiasthmatic property of polyherbal preparation E-721 B. Phytotherapy Research: an International Journal Devoted to Pharmacological and Toxicological Evaluation of Natural Product Derivatives 17 (9), 1092–1097.

Singh, S., Chakaraborthy, G.S., 2020. Evaluation of antiasthmatic and antioxidant potentials of seeds of extract of *Strychnus nuxvomica* L. Research Journal of Pharmacy and Technology 13 (1), 114.

Stevenson, P.C., Kite, G.C., Lewis, G.P., Forest, F., Nyirenda, S.P., Belmain, S.R., Sileshi, G.W., Veitch, N.C., 2012. Distinct chemotypes of *Tephrosia vogelii* and implications for their use in pest control and soil enrichment. Phytochemistry 78, 135–146.

Touqeer, S., Saeed, M.A., Ajaib, M., 2013. A review on the phytochemistry and pharmacology of genus *Tephrosia*. Phytopharmacology 4, 598–637.

Umberto, Q., 2000. CRC world dictionary of plant Names: common names, scientific names, synonyms, eponyms and etymology. MQ. CRC Press 3, 1731p.

Venkatasamy, R., Spina, D., 2016. Novel relaxant effects of RPL554 on guinea pig tracheal smooth muscle contractility. Br J Pharmacol 173 (15), 2335–2351.

Vleggaar Smalberger Thomas, M., Van Aswegen Johannes, L.R., 1978. Flavonoids from *Tephrosia*: part X: the structure of polystachin. S. Afr. J. Chem. 31, 47–50.

Waterman, P.G., Khalid, S.A., 1980. The major flavonoids of the seed of *Tephrosia apollinea*. Phytochemistry 19 (5), 909–915.